Available online at www.sciencedirect.com
SCIENCE DIRECT®
Journal of Chromatography A, 989 (2003) 265–276
JOURNAL OF CHROMATOGRAPHY A
www.elsevier.com/locate/chroma

# Effects of solvent density on retention in gas–liquid chromatography
## II. Polar solutes in poly(ethylene glycol) stationary phases ☆

F.R. González[a,b,*], J. Pérez-Parajón[a]

[a] *Instituto de Química-Física Rocasolano, CSIC, Serrano 119, 28006 Madrid, Spain*
[b] *Div. Química Analítica, Fac. de Ciencias Exactas, Universidad Nacional de La Plata, 47 y 115, 1900 La Plata, Argentina*

Received 14 October 2002; received in revised form 7 January 2003; accepted 7 January 2003

**Abstract**

Effects of solvent density on the solubility of polar probes which undergo specific interactions with poly(oxyethylene) are studied. The analysis of retention data on capillary columns coated with oligomeric poly(oxyethylene) stationary phases shows that, within the experimental error, the enthalpic contribution to the solubility is practically independent of variations in the solvent density. Average values of enthalpies of solute transfer are reported for different probes and temperatures. The observed systematic decrease of solubility with the increasing density is due to a change of entropy. Some thermodynamic consequences inferred from these general results are discussed. One relevant observation is that the influence of solvent's final groups must be negligible. This is even the case for oligomers with number-average degrees of polymerization as low as 13, hosting solutes capable of strong interactions with the end hydroxyl groups of linear poly(ethylene glycols). Possible explanations for this behavior are explored through molecular dynamics simulations of the liquid solvent.


*Keywords:* Density; Partition coefficients; Stationary phases, GC; Thermodynamic parameters; Molecular dynamics; Computer simulations; Poly(ethylene oxide)

## 1. Introduction

Poly(oxyethylene), more trivially named poly(ethylene oxide) (PEO), designates the series of linear polymeric substances with general formula $X–[CH_2–CH_2–O–]_nY$, where X and O–Y are the end-groups and $CH_2–CH_2–O–$ is the repeating structural unit. PEO, either as $–O–CH_3$ terminated polymers derived from glyme (1,2-dimethoxyethane) as the first homologue of the series, or with –OH end-groups derived from ethylene glycol, has found an ample field of applications. Due to its remarkable solubility properties, its low toxicity, good stability and lubricity, is profusely utilized in the petroleum, pharmaceutical, cosmetic and chemical industries. Applications to non-ionic surfactants, tertiary oil recovery and as a drag reduction agent for pumping crude in oil-ducts picture the magnitude of demand and economical importance [1]. In recent years PEO has also gained fundamental academic interest in the ambits of biophysics and biochemistry. The unique

☆ Dedicated to Dr. José Antonio García Domínguez, in memoriam.

* Corresponding author.
*E-mail address:* rex@quimica.unlp.edu.ar (F.R. González).

0021-9673/03/$ – see front matter 
doi:10.1016/S0021-9673(03)00085-2

character of its chain, with its interaction properties, allows to mimic secondary and tertiary structures of biopolymers in different environments [2,3]. The capacity of dissolving salts, forming electrolyte complexes, has drawn interest in electrochemical development as a host polymer matrix for high energy-density batteries [4]. The application to controlled drug-release systems is also under development [5,6]. In the ambit of gas–liquid chromatography (GLC), the melts have been used since a long time as general-purpose polar stationary phases [7].

The cited examples turn almost trivial remarking the importance that acquires the investigation of solubility phenomena on this polymer. Many of the outstanding solubility properties presented by PEO are related to the local conformations of chain segments. Due to the electronegativity of the O atom, the C–O bond has a dipole moment between 0.99 and 1.07 D [8,9], and 1.7 D for the O–H bond. In a given environment (in crystalline solids, amorphous glasses, bulk liquids, or in solution) the polarity is determined by the conformations adopted by chain segments. A chain segment with the dihedral angle O–C–C–O in position *trans* (*t*, 180°) has a lower polarity than the two *gauche* conformations ($g^+$, 60°; $g^-$, −60°). Therefore, polar moieties will present preferential affinity for PEO chain segments having these angles in the *g* state. The direct interrelation existent between polar interactions with other molecules and the predominant local conformations adopted will then determine the global structure of the chain. This in turn will determine other properties, as for example, accessibility of final groups, dependence of melt density with the molar mass, etc. The present body of knowledge concerning the relationship structure/interactions for PEO relies on X-ray diffraction, small-angle neutron scattering, $^{13}$C NMR, conventional IR and Raman spectroscopies and solubility data. These experiments are currently interpreted in conjunction with theoretical studies performed through Monte Carlo and molecular dynamics (MD) simulations, using empirical atomic potential functions (force fields), or either derived from high level ab initio quantum-chemical calculations performed on monomers and dimers (glyme and diglyme) [2,4,10–22].

Through X-ray diffraction analysis of the crystalline solid, a folded structure consisting in a 7/2 helix, with a *tgt* conformation sequence, was postulated [10]. The former specification indicates seven structural units for two helical turns per crystal period, while the latter indicates the conformation of dihedral angles COCC, OCCO and CCOC. Since the all-*trans* sequence *ttt* is expected a priori to be more stable, the apparently paradoxical observation of highly populated *tgt* states in the solid and in solution led to call this phenomenon the ''gauche effect'' [4,11,14,20].

In condensed phases the system partitions into *g* and *t* populations, the relative amount of each depending on temperature, chain-length, and in the case of solutions, also on concentration and solvent nature [15,16]. Karlström [17] has developed a theoretical model that explicitly accounts for this *g*/*t* partitioning of conformer populations. It extends the Flory–Huggins lattice theory for admitting the additional degree of freedom of the chain segments existing in the polar and non-polar conformation, explaining well the phase diagram of PEO–water [19]. It has also been applied to interpret $^{13}$C NMR chemical shift data [18].

In the melt PEO a large *tgt* population is stabilized by the polar intermolecular interactions [16]. The population of the *tgt* conformer decreases with the increasing temperature *T*, favoring the other states. Accordingly, we should expect that the changing polarity with temperature and molar mass should manifest in the solubility phenomena displayed by PEO bulk melts when this is the solvent, as in our particular case of GLC.

Stationary phases in GLC are generally made-up with polymeric materials owing to their low vapor pressure, among other desirable properties. In principle, pure linear polymers constituted by the same structural units, but having different molar mass distributions (MWDs), can be considered neither chemically nor physically the same stationary phase due to several factors. Chemical differences arise from changes in the concentration of final groups, having this factor relevance for oligomers. Distinct physical properties arise from the different average spatial distribution of monomers linked to a different density, as the dimensions and degree of interpenetration of polymer coils varies with their molar masses [23]. For high polymers over a critical molar mass $M_c$, temporal chain linkages originated in chain

entanglements [24,25] introduce another physical variance. Studying the influence on the chromatographic retention of chemical and physical factors, and discriminating between them, could contribute to elucidate some basic questions on the GLC process.

Through the chromatographic determination of alkanes partition coefficients in oligomeric linear poly(ethylene glycols) (PEGs) of different densities (or different MWDs), in a previous paper [26] it was found that the solubility decreases with the increasing solvent density, and that this is a phenomenon originating in a variation of entropy. Changes with the solvent density of solute-transfer enthalpies were observed to be unimportant. The main conclusion was that the solvent-free volume is responsible for this behavior. Another relevant inference drawn from these preliminary results is that the end-groups concentration factor should be of no great concern, because this chemical factor invariably must originate enthalpy differences. This situation could be the consequence of the alkanes' lack of affinity for PEG's end hydroxyl groups, and it may not be the behavior expected for probes capable of strong interactions with –OH. Therefore, to corroborate, or not, the generality of these findings for other solutes and systems arises as an imperative need for adding basic information to our understanding of solubility phenomena and chromatographic retention.

This paper aims at extending the study initiated previously on non-polar alkanes solutes [26] to other solutes capable of specific interactions with PEG stationary phases. Now, our major concern will be focused on trying to elucidate how important are the variations of enthalpy originated by changes in the solvent density (or MWD), and the generality of these behaviors by using different families of probes. We investigate if the decrease of solubility at increasing densities is generally due to a change of entropy and, if this is affirmative, the properties of this dependence.

## 2. General

Assuming that the solubility in oligomeric solvents could generally have a density-dependent contribution, and other roughly density-invariant, implies that this investigation on the GLC retention would demand the discriminative analysis of the transfer enthalpy and entropy, respectively, denoted $\Delta H^*(T)$ and $\Delta S^*(T)$ [27]. These functions correspond to the process of transferring one solute molecule from the ideal gas phase into an infinitely diluted solution in the bulk liquid phase. Since their determination requires evaluating the first derivative $\partial \ln K(T)/\partial T$, the accuracy of modern capillary GLC becomes indispensable for such studies [28]. The partition coefficient $K$ is defined here as the quotient $C_L/C_G$, where $C_L$ and $C_G$ are the number of solute molecules per unit volume (the numeral density), respectively, in the bulk liquid phase and in the gas phase. It is convenient to make a previous overview on the sources of error and to inspect how they impact in the attainment of the thermodynamic functions.

The monitored variable, namely the natural variable of chromatography, is the retention time $t_R$, the retention factor $k$ being the basic measured chromatographic parameter. Measurements of retention factors performed on the same capillary column, under greatly differing operation conditions, yield small standard deviations [29]. For current film thicknesses employed in capillary GLC, $K$ is closely related to the easily measurable apparent partition coefficient $K_{ap}$: $K \approx K_{ap}$ [30]. $K$ being a thermodynamic constant independent of geometric constraints, it allows the comparison of different columns. By definition, the apparent coefficient is:

$$K_{ap} \equiv k\beta = \left(\frac{t_R}{t_M} - 1\right) \cdot \beta \tag{1}$$

$t_M$ is the gas hold-up time and the phase ratio is defined as: $\beta \equiv V_G/V_L$, where $V_G$ and $V_L$ are, respectively, the volumes of gas and liquid phases in the column. Obviously, $\beta$ must be known with exactitude for obtaining $K_{ap}$ reliably.

It has been shown that when the static method of column coating is applied, $\beta$ can be determined exactly from the density of the liquid stationary phase $\rho_L$, and the concentration of the coating solution $C_o$ [26]. Consequently, through appropriate measurement of these, $\beta$ could be attained in principle with the same number of significant digits as for $t_R$ and $t_M$, generally four:

$$\beta(T) = \frac{\rho_L(T)}{C_o} \cdot e^{\alpha_{SiO_2}(T - T_o)} - 1 \tag{2}$$

$T_o$ is the temperature at which the column was filled with the coating solution of concentration $C_o$ and $\alpha_{SiO_2}$ is the volume-thermal-expansion coefficient of the solid capillary wall. For pure silica this is approximately $\alpha_{SiO_2} = 1.96 \times 10^{-6}$ $K^{-1}$ [26], so the exponential factor of Eq. (2) will deviate from unity in the order $10^{-4}$ for the usual chromatographic temperature range. In consequence, this factor can be neglected when $\rho_L$ and/or $C_o$ are given with only three digits.

There is an asymmetric impact on the determination of the thermodynamic functions arising from the error in the absolute value of $\beta$. This error affects $\Delta S^*(T)$, but not $\Delta H^*(T)$ [31]. The reason is that the former function depends on $\ln K(T)$ and its derivative, but the latter only depends on the derivative:

$$\frac{\Delta H^*(T)}{k_B} = T^2 \cdot \frac{\partial \ln K(T)}{\partial T} \quad (3)$$

$$\frac{\Delta S^*(T)}{k_B} = \ln K(T) + \frac{\Delta H^*(T)}{k_B T} \quad (4)$$

where $k_B$ is Boltzmann's constant. While $\Delta S^*(T)$ is affected by the errors on absolute values of measured $k$, $\beta$ and their variation with temperature, $\Delta H^*(T)$ is only affected by the error on the variation $\partial \ln k / \partial T$ and, in a minor degree, by the volume-thermal-expansion of the liquid stationary phase, $\alpha_L$ (see Appendix).

## 3. Experimental

All relevant experimental details concerning the applied chromatographic columns and operation conditions in the present work were presented in Ref. [26]. The calculation procedures employed for $\Delta S^*(T)$ and $\Delta H^*(T)$, through Eqs. (3) and (4), are described in Ref. [28]. The phase ratio has been determined with three significant digits, so this will be the number for $\Delta S^*(T)$. Although four digits are given for $t_R$ and $t_M$, and thus for $k$ (see Eq. 1), since $T$ is provided by the temperature control of the oven with only three, the consequent limitation in the attainment of the derivative, $\partial \ln k / \partial T$, is inevitable.

Table 1 indicates the abbreviations or notations utilized here for designating the studied stationary phases, and a basic characterization of them. As it is shown in the table, the families of studied solutes comprise two homologous series: 1-alkanols and 2-alkanones. Alkylbenzenes starting from toluene to *n*-butylbenzene were also included, as well as pyridine, 1,4-dioxane, 1-nitropropane, benzaldehyde and benzonitrile. Many of these substances were typically utilized in studies of stationary phase selectivity through various methods [7,32–38], all based on linear relationships. Some of these test solutes had been firstly proposed by Rohrschneider [32,33], and were slightly modified afterwards by McReynolds [34]. With adequate solvents, the probes

Table 1
Abbreviations utilized for designating stationary phases and the different families of studied solutes

| Stationary phases | | | Solutes |
|---|---|---|---|
| Designation of the PEG oligomer | Number average degree of polymerization, $\bar{n}_n$ | Density at 100 °C (g/ml) | |
| CW600 | 13 | 1.116 | *Alcohols*: 1-pentanol to 1-decanol |
| M1 (blend of broad MWD) | 15 | 1.108 | *Ketones*: 2-pentanone to 2-octanone |
| M2 (blend of broad MWD) | 18 | 1.088 | *Alkylbenzenes*: toluene to *n*-butylbenzene |
| | | | Benzene |
| | | | Benzaldehyde |
| | | | Benzonitrile |
| CW1000 | 22 | 1.077 | Pyridine |
| | | | 1,4-Dioxane |
| CW1500 | 34 | 1.064 | Nitropropane |

CW is the abbreviation for Carbowax.

set is capable of displaying most current types of interactions in GLC: dipole–dipole interactions (induced and permanent dipoles), π-electron interactions, proton donor–acceptor, etc. Particularly, with the PEG solvents these will be of a widespread variety, complying with one substantial part of our objective: generality.

## 4. Results and discussion

### 4.1. Enthalpy of solute transfer

Using the example of *n*-butylbenzene, Table 2 illustrates the variation of the reduced transfer enthalpy $\Delta H^*/k_B T$ (the enthalpic contribution to $\ln K$, see Eq. (A.1)) found for the different stationary phases, and thus for the changing solvent density. This variation has the same order of the experimental error. Practically the same general behavior is observed for all types of probes. $\Delta H^*$ of them all, polar and non-polar solutes, is generally insensible to variations in the solvent density.

The described experimental fact suggests that the ensemble-average distribution of solvent particles surrounding the solute (which is described by the radial distribution function [39]) should not be altered significantly by the change of stationary phase density. This implies that, close to the solute molecule, the solute–solvent system evolves to nearly the same prevailing lower energy configurations, irrespective of the solvent macroscopic density.

The preceding reasoning is also extensible to the change of concentration of solvent's final groups. For Carbowax (CW) 600, which has a number-average degree of polymerization of 13, the end hydroxyl groups constitute about 6% of the mass of polymer, and reduce to about 2% in CW1500. Since the enthalpy is insensible to the variations of end-groups concentration, even for the stationary phases with lower molar masses and for the solutes that strongly interact with –OH, such as alcohols, we must infer that nearly the same lower energy configurations predominate in all solvents. In other words, the closer coordination spheres around the solute should not be affected considerably by variations of final-groups concentration. This consequence of the experimental observations could seem surprising at first glance, but there might be some specific structural reasons for such a behavior, deserving the correspondent investigation from the molecular viewpoint.

Table 2
Reduced enthalpies of solute transfer, $\Delta H^*/k_B T$, for *n*-butylbenzene at different temperatures

| | 353 K | 373 K | 393 K | 413 K | 433 K |
|---|---|---|---|---|---|
| CW600 | −14.1 | −13.0 | −11.9 | −11.0 | −10.1 |
| M1 | | −13.0 | −11.9 | −11.0 | −10.1 |
| M2 | −14.0 | −12.8 | −11.7 | −10.9 | −10.1 |
| CW1000 | | −13.0 | −11.9 | −10.8 | −10.0 |
| CW1500 | −14.1 | −12.9 | −11.9 | −10.9 | −10.0 |
| Mean value | −14.1 | −12.9 | −11.9 | −10.9 | −10.1 |
| S.D. $\sigma_{n-1}$ | 0.06 | 0.09 | 0.09 | 0.07 | 0.06 |

Table 3 reports the values of $-\Delta H^*/k_B T$ found for all studied solutes, averaged from data taken on the five stationary phases, in the same way as described through the example of Table 2. We shall illustrate two behaviors derived from these results that reveal important general aspects of the solvation process.

Firstly, in Fig. 1 we illustrate the temperature dependence of $\Delta H^*$ for two types of substances. The shape pattern of this function for the rigid heterocy-

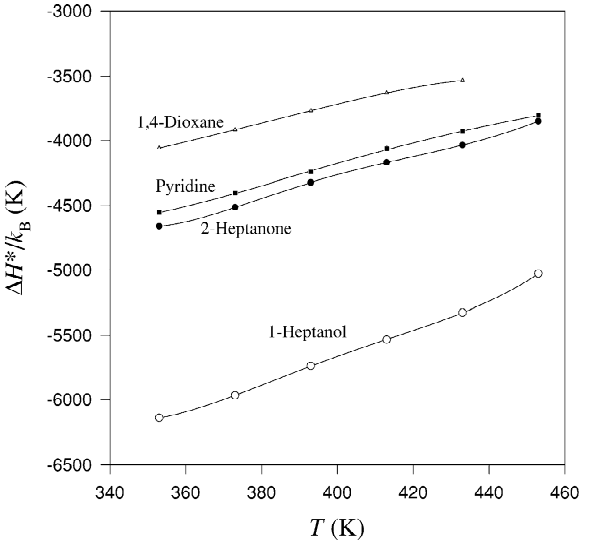


Fig. 1. The behavior with temperature of transfer enthalpies of two rigid heterocycle molecules is compared with that of flexible linear alcohol and ketone molecules.

Table 3
Negative value of the mean reduced enthalpy of solute transfer, $-\langle \frac{\Delta H^*(T)}{k_B T} \rangle$, at different temperatures

| Solute | 353 K | 373 K | 393 K | 413 K | 433 K | 453 K |
|---|---|---|---|---|---|---|
| 1-Pentanol | 15.1 | 13.8 | 12.6 | 11.5 | 10.5 | 9.52 |
| 1-Hexanol | 16.2 | 14.9 | 13.6 | 12.4 | 11.4 | 10.3 |
| 1-Heptanol | 17.4 | 16.0 | 14.6 | 13.4 | 12.3 | 11.1 |
| 1-Octanol | | 17.0 | 15.6 | 14.3 | 13.1 | 12.0 |
| 1-Nonanol | | | 16.6 | 15.3 | 14.0 | 12.8 |
| 1-Decanol | | | | 16.2 | 14.9 | 13.6 |
| 2-Pentanone | 10.8 | 9.85 | 8.97 | 8.21 | 7.59 | 6.88 |
| 2-Hexanone | 12.0 | 11.0 | 10.0 | 9.17 | 8.46 | 7.67 |
| 2-Heptanone | 13.2 | 12.1 | 11.0 | 10.1 | 9.92 | 8.50 |
| 2-Octanone | 14.3 | 13.1 | 12.0 | 11.1 | 10.2 | 9.28 |
| Benzene | 9.98 | 9.10 | 8.23 | 7.51 | 6.99 | 6.39 |
| Toluene | 11.0 | 10.1 | 9.22 | 8.43 | 7.81 | 7.15 |
| Ethylbenzene | 12.0 | 11.0 | 10.1 | 9.25 | 8.54 | 7.82 |
| *n*-Butylbenzene | 14.1 | 12.9 | 11.9 | 10.9 | 10.1 | |
| Benzaldehyde | | 14.7 | 13.5 | 12.5 | 11.5 | 10.6 |
| Benzonitrile | | 15.4 | 14.1 | 13.0 | 12.1 | 11.2 |
| Pyridine | 12.9 | 11.8 | 10.8 | 9.84 | 9.08 | 8.40 |
| 1,4-Dioxane | 11.5 | 10.5 | 9.59 | 8.79 | 8.16 | |
| 1-Nitropropane | 13.3 | 12.2 | 11.2 | 10.2 | 9.44 | 8.67 |

Reported values are the mean of data from the five studied stationary phases. Standard deviations are generally of the order $\sigma_{n-1} < 0.1$.

cles pyridine and 1,4-dioxane clearly differs from that of the linear flexible molecules of the plotted aliphatic alcohol and ketone. Based on elementary physical notions, some features of these observations should be expected a priori.

Along with the analysis of different experimental and theoretical issues, it has been discussed earlier [28,39,40] that the contribution from the internal degrees of freedom of the solute molecule to the heat capacity of transfer, $\Delta C_p^*$, is a determinant factor affecting the temperature dependence of solvation.[1] Since $\Delta C_p^* = \partial \Delta H^* / \partial T$, the reduced heat capacity $\Delta C_p^*/k_B$ is the slope of tangents to the curves plotted in Fig. 1. Sufficiently long linear flexible molecules generally present two maximums of $\Delta C_p^*(T)$ in the chromatographic range of $T$ [26,41]. One maximum, or more precisely the band associated with it, would correspond to the solute's backbone bending vibration modes [28]. In the case of the rigid cycles, such low-energy bending motions are less important, so a smoother $\Delta H^*(T)$ curve is expected with respect to the linear flexible ones (one inflexion point could remain unobservable).

The second aspect of interest concerns the isothermal chain-length dependence of $\Delta H^*$ for homologous series. Fig. 2 illustrates the behavior of the reduced enthalpy using the example of the normal alcohols series. Within the experimental error, we can assume the isotherm $\Delta H^*(n)$ as linear. This behavior contrasts with the non-linear one of ln $K(n)$ shown in Fig. 3, using data from a single column, and reveals that the curvature of the latter isotherm must be originated by entropic effects. The same results are observed for *n*-alkanes solutes [41].

The entropic origin for the non-linear behavior of ln $K(n)$ has been anticipated through simple theoretical arguments, ascribing it to the free-volume entropy $\Delta S_{fv}$ [39]. This contribution to $\Delta S^*$ is given by:

$$\frac{\Delta S_{fv}}{k_B} = \ln \frac{V_f}{V_L} \tag{5}$$

where $V_f$ is the free-volume in the liquid solution. The reason why $\Delta S_{fv}$ is not a linear function of $n$ is that the excluded volume of short chain molecules

[1] We must also consider for PEG the population decrease with $T$ of the more polar *tgt* conformational states, but this would only introduce a monotonous increase of $\Delta H^*$ for polar solutes.

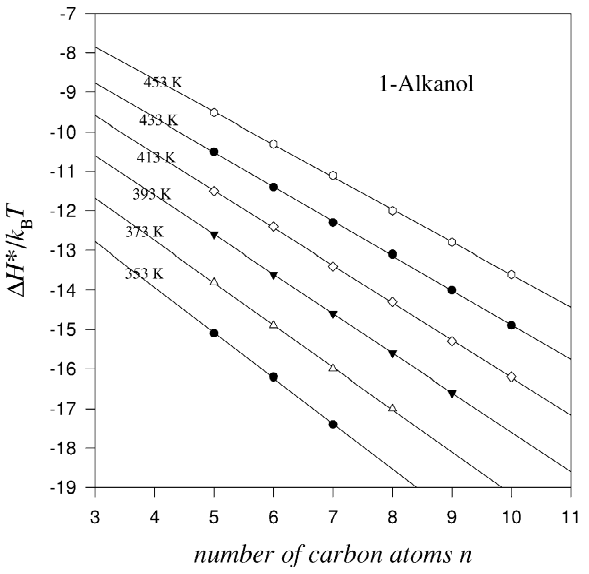


Fig. 2. Isotherms of the reduced transfer enthalpy are plotted as function of the number of carbon atoms in 1-alkanols. The best curve-fit corresponds to a linear behavior.

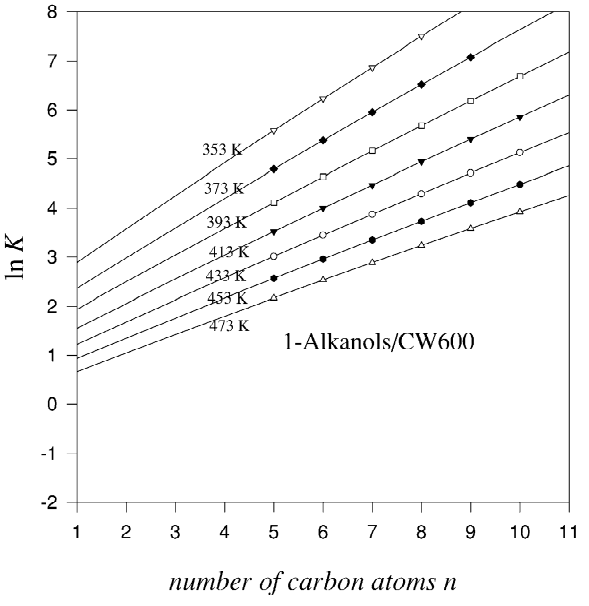


Fig. 3. Isotherms of $\ln K$ are represented as function of number of carbon atoms in the normal alcohol series, using data from a single column. The behavior is non-linear.

does not grow linearly with the number of monomers; it scales as $n^{\delta}$, with $\delta \sim 2$ (the excluded volume fraction in the solution is $1-(V_f/V_L)$).

There was also some theoretical expectance for the linearity of $\Delta H^*(n)$, at least for the contributions from the solute. Monte Carlo studies of the internal energy of chain molecules placed in different generic environments, as for example poor solvents and good solvents, have shown that this is a linear function of the chain length [42]. Then, the difference of energies between two different environments, in our case involving the solute transfer process from the gas to the liquid phase, must be linear. Only the internal energy of transfer $\Delta E^*$ is the important contribution to $\Delta H^*$, since $p\,\Delta V^*$ is generally about $10^{-3}$ of the order of $\Delta E^*$ [27,43]:

$$\Delta H^* = \Delta E^* + p\,\Delta V^* \approx \Delta E^* \quad (6)$$

The difference of Helmholtz's free energy is the main driving force for most solvation processes of small molecules at infinite dilution. From the above considerations, constancy of $\partial \Delta H^*/\partial n$ with respect to the solute contributions (the work of cavity formation is not being contemplated) should be expected a priori.

### 4.2. Entropy of solute transfer

It is observed for all types of probes that the solubility decreases with the increasing solvent density. According to the results of Section 4.1 the approximate relationship $\partial \Delta H^*/\partial \rho_L \approx 0$ holds as a general rule, so it becomes obvious that the decrease of solubility must be originated in entropy effects. Nevertheless, we should analyze also if the influence of the variables on this entropic change follow the same patterns observed for alkanes, in order to evaluate probable molecular mechanisms responsible for this behavior.

In the previous paper [26] it was shown that the variation $\partial \ln K/\partial \rho_L$ was rather insensitive to temperature and the alkane molar masses. The same applies to the variation with density of $\Delta S^*$, since the decrease of $\ln K$ was due to this factor. With the aim of corroborating if these features are general ones, in Fig. 4 we illustrate the behavior found for different probes at different temperatures. In place of

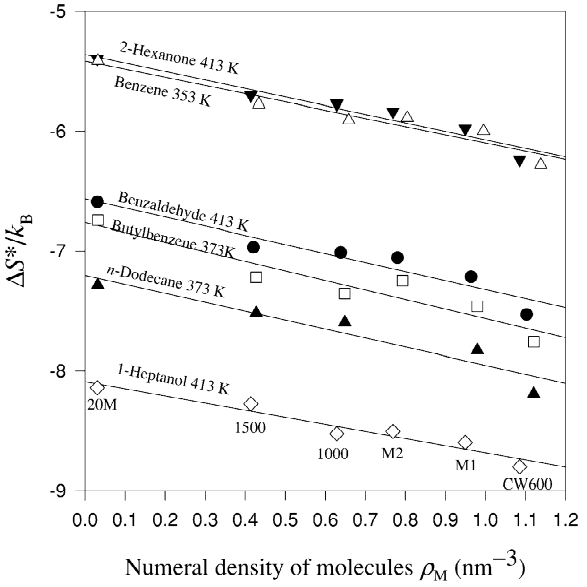


Fig. 4. Dependence of the reduced transfer entropy with the number of molecules per cubic nanometer, for different probes and temperatures. The variation $\partial\Delta S^*/k_B\partial\rho_M$ is rather insensible to the nature of probes and *T*.

the solvent density $\rho_L$, the selected variable for plotting the results is the average numeral density of molecules, $\rho_M$, expressed as the number of molecules per cubic nanometer. The abscissa was calculated according to $\rho_M = \underline{\rho}_L \; N_A/\overline{M}_n$, where $N_A$ is Avogadro's number and $\overline{M}_n$ is the number-average molar mass of the stationary phase. This variable provides a smoother correlation, facilitating the presentation and comparisons of results. Data for Carbowax 20M were included. These were calculated from values of *K* reported by Poole et al. [7], by applying Eq. (4) and using the average $\Delta H^*$ of Table 3.

We can see in Fig. 4 that probes of very different chemical nature, at different temperatures, yield similar behaviors. Basically, the same features as for alkanes are observed. Some doubt persists on the precise nature of this dependence on the variables of the solvent. However, it can be assumed $\partial\Delta S^*/\partial\rho_M \approx$ const. in oligomeric PEG solvents as a general approximate condition. This variation, averaged over different temperatures and probes, has the order: $\partial\Delta S^*/k_B\partial\rho_M \approx -0.7$ nm$^3$.

## 5. Further remarks

We must be aware that the preceding results correspond to oligomeric solvents well below the critical chain length for the occurrence of chain entanglements, $M_c$ [25,26], and there are no precedents studying solvation differences between temporarily linked chain networks and the more freely moving oligomeric chains.

The described behaviors of $\Delta H^*$ and $\Delta S^*$ with $\rho_L$ seem to have a general character, considering the dissimilar chemical and structural nature of the probes employed in this study, and the consequent variety of interactions taking place with the liquid. Notwithstanding, it might not be expected universality arguing the specificity originated by the unique characteristics of the solvent. For example, the decrease of PEG's density by increasing $\overline{M}_n$ [26] and the *gauche* effect are quite atypical properties for a linear polymer. But the variation of $g/t$ populations with the molar mass distribution of the employed stationary phases, and its associated change of polarity, has not any observable important consequence on $\Delta H^*$. Therefore, this particular structural feature of PEO is not relevant for our concern and we can fairly presume universality for the insensible behavior of $\Delta H^*$ toward variations in the macroscopic density of linear oligomers.

Generally speaking, the presence of final groups in polymer solvents should have a small impact on solvation, due to the low concentrations currently found for these structural entities. However, in the case of the studied PEG oligomers, the strength of the interaction between hydroxyl groups and their concentration level in the stationary phases with lower $\overline{M}_n$ should create expectation on a significant $\partial\Delta H^*/\partial\rho_L < 0$ for alcohols solutes. But we must be aware that if folded molecular conformations predominate in liquid PEG, which is one plausible explanation for the observed decrease of $\rho_L$ with $\overline{M}_n$ [26], molecules could adopt structures such that the end groups would not be readily accessible for interactions with the solute. Also, the final –OH could be compromised with intramolecular H-bonding, or just strong attractive interactions, leading to lower free energies than those of conformations required for the occurrence of intermolecular interactions.

The verisimilitude of the formulated hypotheses can be explored through molecular modeling. In fair approximation, low-frequency molecular motions are describable through classical calculations. These can provide qualitative information that may be useful for answering specific questions on conformational properties of the liquid.

## 6. Molecular dynamics simulations

Our circumstantial interest is focused on the prevailing conformations of PEG in the bulk liquid and particularly on those involving the final groups. With this purpose we have implemented molecular dynamics simulations of the liquid PEG using the commercial software Hyper Chem (Hypercube, Ontario, Canada) [44].

A cubic periodic box was built with 35-Å sides, containing 48 linear PEG molecules of 13 structural units each, thus resembling the number-average degree of polymerization of CW600. This system also reproduces the experimental macroscopic density of the oligomer at 393 K, with a density $\rho_L =$ 1.098 g/ml [26]. The starting structure of the molecules was the extended chain with all OCCO torsion angles in *trans*. In the simulation the central box is surrounded by 26 identical boxes, which are its translated image, so 1296 total molecules are involved. The all-atoms AMBER empirical force field was employed, which has a refinement for H-bonding distances [44,45]. Truncation of the non-bonded pair potential functions was applied through switched functions. These provided a smooth turn-off of the non-bonded interactions at interatomic distances between 10 and 14 Å.

In order to overcome the potential energy barriers, the system was initially heated at 593 K for 100 ps, using a time step of 1 fs and a simulated thermostatic bath with a relaxation time of 0.1 ps [44,46], until steady state was reached. It was then cooled down, in the same conditions, to 393 K in two steps. A simulation of 300 ps at 393 K was then performed without the thermostatic bath. Once the box became equilibrated, conformational sampling during a 100-ps simulation was carried out for the calculation of ensemble-averages on several parameters. These averages correspond to the microcanonical ensemble, i.e., the constant number of molecules, volume and energy thermodynamic environment (*N*, *V*, *E*). The average end-to-end molecular distance of the sampled molecules yielded $\langle r^2\rangle^{1/2} = 22.2$ Å. This distance renders a characteristic ratio of $C_n = 5.7$, where $C_n = \langle r^2\rangle / \Sigma n_i \, l_i^2$, being $n_i$ and $l_i$, respectively, the number of backbone bonds and their length, for the different types i. This value lies in-between $C_n = 4.9$ for tetraglyme at 300 K [4] and $C_\infty = 5.6$–$6.3$ for a high molar mass polymer at 390 K, determined through small-angle neutron scattering [12]. It is slightly greater than that taking place in theta solutions of the polymer [12] (at the $\Theta$ temperature folded molecular conformations are adopted). In Fig. 5a a snapshot of the equilibrated box is represented. Only one molecule from the snapshot is displayed in Fig. 5b using a ball-stick rendering. This figure illustrates the type of structures adopted by the chains. The *g* was the most populated state for the OCCO torsion angles, with a total fraction of 0.80 (only a 0.20 fraction of *trans*), so the simulation correctly accounts for the *gauche* effect. The applied criterion for classifying the angles was assuming *g* when abs($\phi$)$<$120°, and *t* when abs($\phi$)$\geq$120°, $\phi$ being the angle.

For the final OCCO dihedral angles, those involving the end –OH groups, the most populated was also the *g* state. This constituted an average fraction of 0.83. The H$\cdots$O average distance of atoms 1–5 for these conformers was 3.2 Å, and the average angle was 67°. This fact indicates that the final –OH has only a very weak 1–5 intramolecular H$\cdots$O attractive interaction. Solely the interactions 1–5 (i.e., the ''pentane effect'') were found to be significant. Interactions of longer range (1–8, 1–11, etc.), namely those of the end –OH with inner chain segments, were not significant.

Fig. 6 is a snapshot representing the end-groups distribution of all molecules. One end-O was selected as the ''central'' and the distance to its closer end-H neighbors was averaged during the simulation, determining the average time the O$\cdots$H distance, $d_{O\cdots H}$, was shorter than 3 Å. The calculation was performed over a sample of ''central ends'' yielding the following results: average fraction of time spent in interaction ($d_{O\cdots H} < 3$ Å) = 0.48; average $d_{O\cdots H}$ during the interaction = 2.3 Å. These results indicate

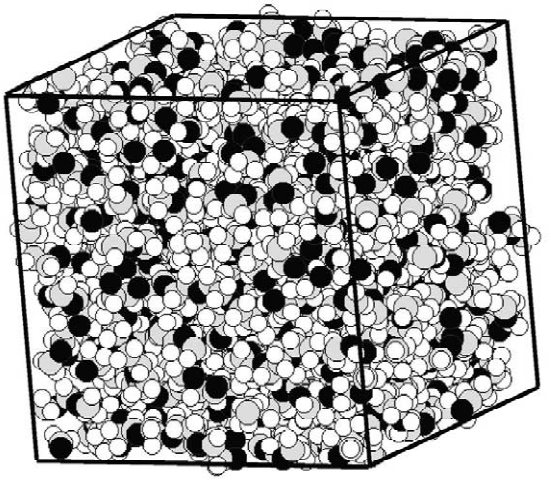

(a)

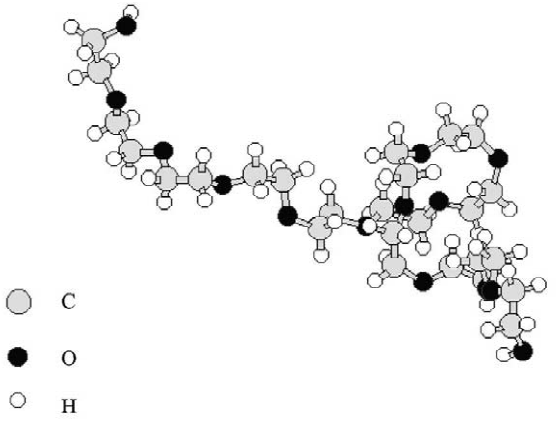


(b)

Fig. 5. (a) Snapshot of an equilibrated periodic box at 393 K. The box contains 48 PEG molecules of 13 structural units each. The density of the box is the same as the experimental macroscopic one of CW600. (b) Snapshot representation of a single molecule from (a). The molecular coil adopts a rather folded structure, whose dimensions are slightly more extended than those in Θ solutions.

that intermolecular interactions of final –OH groups are rather more effective than the 1–5 intramolecular ones.

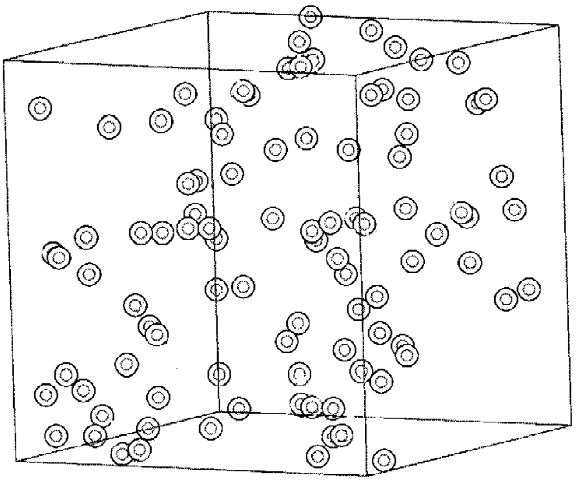

Fig. 6. Snapshot showing the distribution of final groups.

## 7. Conclusions

For solutes of very different chemical and structural nature the enthalpic contribution to their solubility in PEG linear oligomers is practically independent of the solvent density or MWD. The observed decrease of solubility with the increasing solvent density is due to the effect of entropy, probably a consequence of the decrease in the solvent free-volume. If $\partial \Delta S^*/\partial \rho_M$ is originated in the variation of the solvent free-volume, its insensible behavior with $T$ can be explained by the low temperature variation of $\langle r^2 \rangle^{1/2}$ [46].

We conclude that the solute–solvent system evolves to nearly the same lower energy configurations of solvent particles surrounding the solute, irrespective of the macroscopic density, the concentration of final groups and the populations of polar conformers in the PEG solvent. Linear polymers below $M_c$, having different MWDs, can be considered essentially the same stationary phase because their retention only differs in a factor that is insensible to temperature, whose effect is not very different than that resulting form a change in the column phase ratio.

For any homologous series of solutes having an aliphatic chain, $\Delta H^*$ is a linear function of the number of methylene units in the solute molecule.

The curvature observed for the isotherm $\ln K(n)$ is also due to the effect of entropy. Summarizing, the entropy of solute transfer is responsible for both non-linear structural effects and the variation of solubility with the density of particles in the stationary phase. Therefore, for linearly based empirical structure–retention studies, in which the polymeric solvent is characterized only generically, it would be rather more appropriate to use $\Delta H^*/k_B T$ as the correlating variable in place of $\ln K$ or any other associated parameter.

MD simulations show that the insensible behavior of $\Delta H^*$ toward the variation of end-groups concentration seems not to be explainable through the compromise of the end –OH in intramolecular interactions.

**Acknowledgements**

This work was sponsored by Consejo Superior de Investigaciones Científicas of Spain (CSIC), project PB 98-0537-C02-01. F.R.G. is holder of an external fellowship from Consejo Nacional de Investigaciones Científicas y Técnicas of Argentina (CONICET) at Instituto de Química-Física ''Rocasolano'', Madrid, Spain.

## Appendix

The Gibbs free energy of solute transfer, $\Delta G^*$, is related to the gas/bulk-liquid partition coefficient at infinite dilution, $K$, through [27]:

$$\ln K = \frac{-\Delta G^*}{k_B T} = \frac{\Delta S^*}{k_B} - \frac{\Delta H^*}{k_B T} \quad (A.1)$$

The basic relationship $\Delta S^* = -(\partial \Delta G^*/\partial T)_p$ then states that the thermodynamic functions are related to the experimentally measurable $K$ through:

$$\frac{\Delta S^*(T)}{k_B} = \ln K(T) + T\frac{\partial \ln K(T)}{\partial T} \quad (A.2)$$

$$\frac{\Delta H^*(T)}{k_B} = T^2\frac{\partial \ln K(T)}{\partial T} \quad (A.3)$$

In the usual chromatographic conditions $K$ does not depend significantly on the pressure $p$ [29], so in the above given expressions it is unnecessary to indicate the constancy of $p$. The directly measurable parameters in capillary GLC are $k$ and $\beta$, then, the introduction of Eq. (1) into Eqs. (A.2) and (A.3) yields:

$$\frac{\Delta S^*}{k_B} = \ln k + \ln \beta + T\left(\frac{\partial \ln k}{\partial T} + \frac{\partial \ln \beta}{\partial T}\right) \quad (A.4)$$

$$\frac{\Delta H^*}{k_B} = T^2\left(\frac{\partial \ln k}{\partial T} + \frac{\partial \ln \beta}{\partial T}\right) \quad (A.5)$$

The variation of $\ln \beta$ with $T$ can be estimated through Eq. (2), taking into account that it is generally $\rho_L/C_o \gg 1$ and that $C_o$ is a constant independent of $T$:

$$\frac{\partial \ln \beta}{\partial T} \approx \frac{\partial \ln \rho_L}{\partial T} + \alpha_{SiO_2} = \alpha_{SiO_2} - \alpha_L \quad (A.6)$$

The same relationship can be derived straightforwardly from the definition of $\beta$, approximating the volume of the gas phase, $V_G$, to the internal volume of the capillary column, $V_C$. This physical approximation is the one implicit in neglecting 1 with respect to $\rho_L/C_o$ in Eq. (A.6).

Due to the fact that the thermal expansion of the liquid stationary phase is much greater than that of the solid silica wall of the capillary, the phase ratio decreases with an increment of temperature proportionally to the volume-thermal-expansion coefficient of the liquid, $\alpha_L$. In consequence, we see that beside the experimental error on $\partial \ln k/\partial T$, mainly associated with the imprecision of the thermal control of the oven in the chromatograph, the determination of $\Delta H^*(T)$ is also affected by $\alpha_L$. The latter can be determined accurately by pycnometry and it is found to vary, for PEGs of different MWDs, in the range: $\alpha_L = 7.8–9.5 \times 10^{-4}$ $K^{-1}$ [26].

## References

[1] F.E. Bailey, J.V. Koleske, in: Polyethylene Oxide, Academic Press, New York, 1976.
[2] S. Magazù, J. Mol. Struct. 523 (2000) 47.
[3] K. Devanand, J.C. Selser, Nature 343 (1990) 6260.
[4] H. Dong, J. Hyung, C. Durham, R.A. Wheeler, Polymer 42 (2001) 7809.

[5] B.A. Ferreira, H.F. Dos Santos, A.T. Bernardes, G.G. Silva, W.B. De Almeida, Chem. Phys. Lett. 307 (1999) 95.
[6] A. Apicela, B. Capello, M.A. Del Nobile, M. La Rotonda, G. Menisitieri, L. Nicolais, S. Seccia, in: Polymeric Drugs and Drug Administration, American Chemical Society, Washington, DC, 1994.
[7] C.F. Poole, Q. Li, W. Kiridena, W.W. Koziol, J. Chromatogr. A 898 (2000) 211.
[8] Flory, in: Statistical Mechanics of Chain Molecules, Interscience, New York, 1969.
[9] A. Abe, J. Mark, J. Am. Chem. Soc. 98 (1976) 6468.
[10] Y. Takahashi, H. Tadokoro, Macromolecules 6 (1973) 672.
[11] F. Müller-Plathe, W.F. van Gunsteren, Macromolecules 27 (1994) 6040.
[12] G.D. Smith, D.Y. Yoon, R.L. Jaffe, R.H. Colby, R. Krishnamoorti, L.J. Fettes, Macromolecules 29 (1996) 3462.
[13] G.D. Smith, D.Y. Yoon, C.G. Wade, D. O'Leary, A. Chen, R.L. Jaffe, J. Chem. Phys. 106 (1997) 3798.
[14] G.D. Smith, O. Borodin, M. Pekny, B. Annis, D. Londono, R.L. Jaffe, Spectrochim. Acta Part A 53 (1997) 1273.
[15] G.D. Smith, D. Bedrov, O. Borordin, J. Am. Chem. Soc. 122 (2000) 9548.
[16] M. Rozenberg, A. Loewenschuss, Y. Marcus, Spectrochim. Acta Part A 54 (1998) 1819.
[17] G.J. Karlström, J. Phys. Chem. 89 (1985) 4962.
[18] M. Björling, G.J. Karlström, P. Linse, J. Phys. Chem. 95 (1991) 6706.
[19] O. Engkvist, G. Karlström, J. Phys. Chem. B 101 (1997) 1631.
[20] S. Neyertz, D. Brown, J.O. Thomas, J. Chem. Phys. 101 (1994) 10064.
[21] S. Neyertz, D. Brown, J. Phys. Chem. 102 (1995) 9725.
[22] S. Neyertz, D. Brown, J.H. Clarke, J. Chem. Phys. 105 (1996) 2076.
[23] P.J. Flory, in: Principles in Polymer Chemistry, 7th edition, Cornell University Press, New York, 1969.
[24] J.D. Ferry, in: Viscoelastic Properties of Polymers, 3rd edition, Wiley, New York, 1980.
[25] W.W. Graessley, Adv. Pol. Sci. 16 (1974).
[26] F.R. González, J. Pérez-Parajón, J.A. García-Domínguez, J. Chromatogr. A 953 (2002) 151.
[27] A. Ben Naim, in: Solvation Thermodynamics, Plenum Press, New York, 1987.
[28] F.R. González, J. Chromatogr A 942 (2002) 211.
[29] F.R. González, L.G. Gagliardi, J. Chromatogr. A 879 (2000) 157.
[30] F.R. González, R.C. Castells, A.M. Nardillo, J. Chromatogr. A 927 (2001) 111.
[31] F.R. González, A.M. Nardillo, J. Chromatogr. A 779 (1997) 263.
[32] L. Rohrschneider, J. Chromatogr. 22 (1966) 6.
[33] L. Rohrschneider, Adv. Chromatogr. 4 (1967) 333.
[34] W.O. McReynolds, J. Chromatogr. Sci. 8 (1970) 685.
[35] L.R. Snyder, J. Chromatogr. Sci. 16 (1978) 223.
[36] B.R. Kersten, S.K. Poole, C.F. Poole, J. Chromatogr. 468 (1989) 235.
[37] J. Li, A.J. Dallas, P.W. Carr, J. Chromatogr. 517 (1990) 103.
[38] J. Li, Y. Zhang, P.W. Carr, Anal. Chem. 64 (1992) 210.
[39] F.R. González, J.L. Alessandrini, A.M. Nardillo, J. Chromatogr. A 852 (1999) 583.
[40] F.R. González, A.M. Nardillo, J. Chromatogr. A 842 (1999) 29.
[41] F.R. González, J. Pérez-Parajón, J. Chromatogr. A (2003) in press.
[42] O. Collet, S. Premilat, Macromolecules 26 (1993) 6076.
[43] J. Tomasi, M. Persico, Chem. Rev. 94 (1994) 2027.
[44] HyperChem manuals: Computational Chemistry, Reference Manual, Hypercube, 1996.
[45] S.J. Weiner, P.A. Kollman, D.T. Nguyen, D.A. Case, J. Comp. Chem. 7 (1986) 230.
[46] C. Sarmoria, D. Blankschstein, J. Phys. Chem. 96 (1992) 1978.